EUROPEAN ORGANIZATION FOR NUCLEAR RESEARCH

Proposal to the ISOLDE and Neutron Time-of-Flight Committee

Investigating shape coexistence in ^{80,82}Sr with β^{+}/EC decay spectroscopy

September 24, 2020

N. Bernier[1,2], T. D. Bucher[1,2], J. N. Orce[1], L. J. Evitts[3], T. Kibédi[4], P. E. Garrett[5,1], T. R. Rodríguez[6], K. J. Abrahams[1], E. H. Akakpo[1], A. Algora[7], A. Andreyev[8], H. Bidaman[5], V. Bildstein[5], M. J. G. Borge[9], S. Buck[5], A. Briscoe[10], J. A. Briz[9], K. Chrysalidis[15], J. Cubiss[6], L. M. Fraile[11], J. Henderson[12], A. Illana[10,13], D. G. Jenkins[8,1], A. Korgul[14], R. Lica[15], C. V. Mehl[1], K. Miernik[14], A. I. Morales[5], E. Nácher[5], C. Ngwetsheni[1], S. S. Ntshangase[2], J. Ojala[10], B. Olaizola[15], S. Orrigo[5], R. Page[16], J. Pakarinen[10], M. Piersa[14], A. Radich[5], S. Rothe[15], B. Rubio[7], J. Smallcombe[16], M. Stryjczyk[17], S. Triambak[1], S. Valbuena[5], R. Wadsworth[8], and the IDS/ISOLDE Collaboration

[1] *University of the Western Cape, South Africa*
[2] *University of Zululand, South Africa*
[3] *Bangor University, United Kingdom*
[4] *Australian National University, Australia*
[5] *University of Guelph, Canada*
[6] *Universidad Autónoma de Madrid, E-28049 Madrid, Spain*
[7] *Instituto de Física Corpuscular, CSIC - Univ. Valencia, Spain*
[8] *University of York, United Kingdom*
[9] *CSIC, Madrid, Spain*
[10] *University of Jyväskylä, Finland*
[11] *Universidad Complutense de Madrid, Spain*
[12] *University of Surrey, United Kingdom*
[13] *Helsinki Institute of Physics, Finland*
[14] *University of Warsaw, Poland*
[15] *CERN, Switzerland*
[16] *University of Liverpool, United Kingdom*
[17] *KU Leuven, Belgium*

CERN-INTC-2020-071 / INTC-P-586
24/09/2020

Spokespersons: Nikita Bernier nbernier@alumni.ubc.ca,
Thifhelimbilu Daphney Bucher daphney52@gmail.com,
Nico Orce jnorce@uwc.ac.za

Contact person: Razvan Lica razvan.lica@cern.ch

Abstract: Neutron deficient ^{80,82}Sr nuclides lie in a rich structural region of the nuclear chart, where sub-shell effects may give rise to rapid shape changes. Large $E0$ strengths, $\rho^2(E0)$, are related to fluctuations in the mean-square charge radius, $\langle r^2 \rangle$, and typically associated with coexisting shapes which become mixed. Although the structure of yrast states in this region is well known from heavy-ion fusion-evaporation reactions – where a shape evolution from spherical at $N = 50$ to strongly deformed in the $N \leqslant 40$ region has been observed as a function of spin – information of non-yrast states remains scarce. Currently, there are no data on excited 0^+ states for ^{80}Sr and little information on $E0$ strengths, in general. Excited 0^+ states can, however, be populated through β-decay and Coulomb-excitation studies. Here, we propose the investigation of shape effects in ^{80,82}Sr with the β^+/EC decay of ^{80,82}Y and with the measurement of internal conversion electrons using the SPEDE electron spectrometer at the ISOLDE Decay Station (IDS), equipped with a tape station, four germanium clover detectors, two $LaBr_3$(Ce) detectors, and a fast plastic detector. These measurements will complement the investigation of the shape effects in ^{80,82}Sr using safe multi-step Coulomb excitation measurements carried out at TRIUMF, where the excited 0_2^+ state has been populated in ^{82}Sr.

Requested shifts: 19 shifts (split into 2 runs over 1 year)

1 Physics Motivation

Strontium isotopes lie in a particularly rich region of the nuclear landscape, where a variety of subshell gaps may give rise to sudden changes in deformation. The neutron-deficient isotopes $^{76-82}$Sr are found to have anomolous ground-state rotational bands with large $E2$ strengths [1, 2, 3, 4, 5, 6]. The relationship between light strontium isotopes' large $E2$ strengths and $R_{4/2} = E(4_1^+)/E(2_1^+)$ values deviate from that which would be expected as nuclei evolve into an axially symmetric rotor (see Fig. 1). This behaviour can be explained by softness of the potential energy surface or by shape coexistence, the identification of which is the purpose of the present submission. It is proposed to take advantage of the significant yields of neutron-deficient yttrium isotopes which can be produced at the ISOLDE facility and decays to populate the excited states of strontium isotopes, of particular interests are ^{80}Sr and ^{82}Sr. Nuclei in the vicinity of the $N = Z$ line are also of considerable astrophysical interest since recent rp-process nucleosynthesis simulations for X-ray bursts and X-ray pulsars are strongly dependent on nuclear structure effects. The mass 80 nuclei are crossed by various scenarios of the rp-process nucleosynthesis and β-decay rates and nuclear deformations have a strong impact not only on the reaction path but also on the calculated production rates [7].

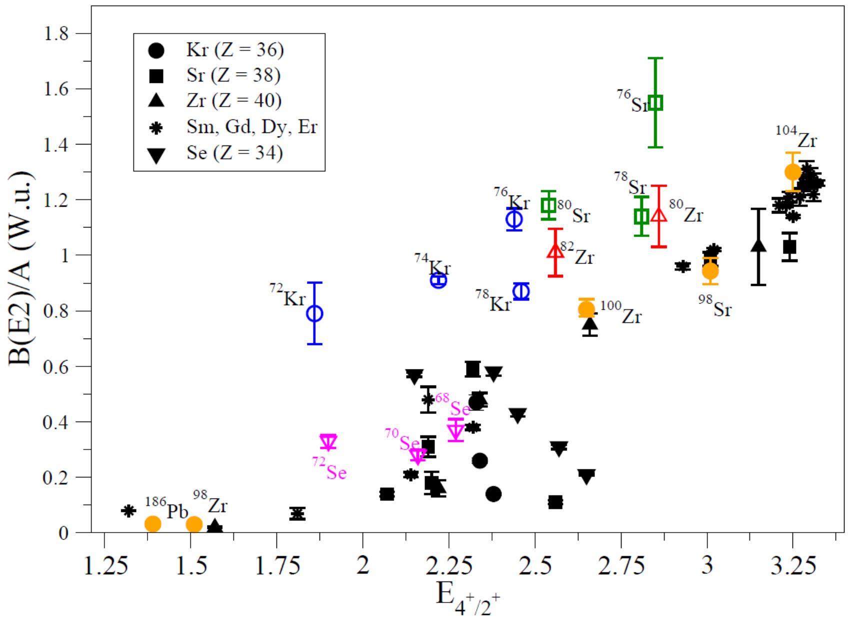

Figure 1: $B(E2)$ values normalised for A, plotted against $R_{4/2} = E(4_1^+)/E(2_1^+)$ values. Neutron-deficient strontium isotopes exhibit a similar behaviour to other known shape-coexisting nuclei.

The Nilsson diagram for neutron and proton single-particle states in the region of interest [8] is shown in Fig. 2, highlighting the various possible shape minima in this area of the nuclear landscape. Shape-coexistence is often indicated by the existence of low-lying excited 0^+ states, as have been observed in the neutron-deficient Se [9, 10, 11] and Kr isotopes [12, 13, 14]. As yet, no such states have been identified in ^{76,78}Sr, which are predicted to have prolate ground-state deformations [15]. Shape coexistence is predicted

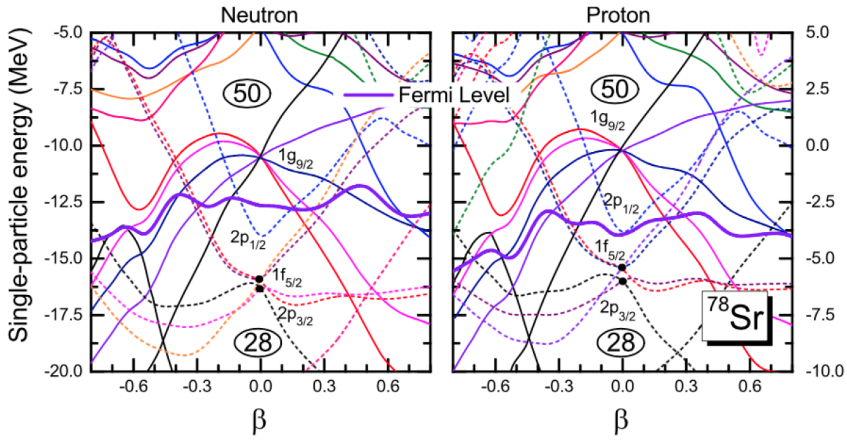

Figure 2: Deformed single-proton and -neutron energies in the region of interest [17]. The Fermi surface for ^{78}Sr is indicated by the thick purple line.

to manifest in the light strontium isotopes; EXCITED VAMPIR calculations [16] predict an oblate band built on the 0^+_2 state at 0.5 MeV in ^{76}Sr, whilst for ^{78}Sr, excited prolate and oblate bands are predicted above the prolate ground state, with the band heads lying at 2.5 and 3 MeV, respectively. In the case of ^{80}Sr, a 0^+_2 state has tentatively been assigned from a (^{3}He,n) measurement, lying at $\sim$ 1 MeV, as shown in Fig. 3. Such states would likely be observed in β-decay studies with the use of the electron spectrometer SPEDE. In general, large $E0$ matrix elements are related to changes in the quadrupole deformation [19]. A large electric monopole strength, $\rho^2(E0)$, is expected whenever configurations with different mean-square charge radii mix [18, 19]. Hence, the identification of these excited 0^+ states in a chain of isotopes allow to study the evolution of the nuclear shape at low spins.

Recent total-Routhian-surface calculations [21] predict a very narrow separation of less than 220 keV between prolate and oblate shape minima in ^{80}Sr. A γ-band has previously been identified in ^{80}Sr from a β^+/EC decay study of ^{80}Y [6, 7], with a bandhead observed at 1141 keV, as shown in Fig. 4. No transition strengths were determined in these studies. In the case of the neutron-deficient strontium isotopes, triaxiality may well be an important degree of freedom, and the accurate determination of the $E2$ strengths in the γ-band is relevant to investigate the systematics of γ-bands in this region. These will then be compared with those of heavier axially-symmetric and γ-soft rotors, where a systematic behaviour has been observed with $B(E2; 2^+_\gamma \rightarrow 0^+_1)$ values between 1-7 W.u. and tens of W.u., respectively. A study of triaxiality by Bonche et al. [22] predicted γ-softness in the ground states of a number of neutron-deficient Zr, Sr and Kr isotopes. Of the light strontium isostopes, only ^{76}Sr was predicted to have a well-defined prolate minimum, with ^{80}Sr being extremely γ-soft and predicted to have a triaxial ground state.

2 Experimental Method

β-decay studies are a powerful tool for investigating shape-effects in nuclei. It is proposed to use the ISOLDE mass separated radioactive beam, to populate the non-yrast low-

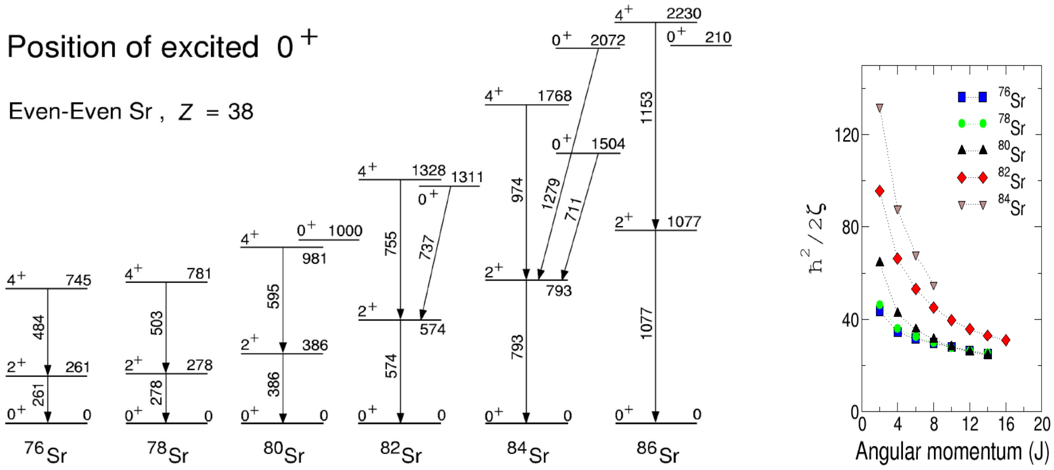

Figure 3: The excited 0^+ states and the yrast excitation levels for the strontium isotopes. No $E0$ transition has previously been observed. In ^{80}Sr, there has been no evidence of a transition from the excited 0^+ to the 2_1^+ state. However, it is expected to be observed in the proposed measurement. Figure modified from Ref. [23]. The right panel shows the anomalous rotational behaviour of the 2_1^+ states in the Sr isotopes, often associated with shape coexistence.

lying excited states in ^{80,82}Sr via the β-decay of ^{80,82}Y (see Fig. 3). These measurements will complement the investigation of the shape effects in ^{80,82}Sr using the safe multi step Coulomb excitation experiments approved with high priority at TRIUMF with the TIGRESS spectrometer. The ^{82}Sr part of the campaign was conducted in July 2018, where the excited 0_2^+ state has been populated.

The $E0$ transition strength will be used as an indication of shape coexistence and a probe for shape evolution. We are proposing to populate the excited 0^+ states by β^+/EC decay. For ^{82}Sr, the second 0^+ excited state at 1310.8 keV (shown in shown in Fig. 5) is populated with a combined β^+/EC feeding intensity of 2.121% from the 1^+ ground state of ^{82}Y (allowed transition). For ^{80}Sr, there is no published value, however it is expected to be populated in the proposed decay measurement by the (1^-) isomer in ^{80}Y that has a half-life of 4.8(3) s and a measured β^+/EC branch of 19(2)%.

In order to estimate the rate of electrons observed in the $E0$ transitions, we first estimate a value of $q^2(E0/E2)$, which is the intensity ratio between the $E0$ transition, and the competing $0_2^+ \rightarrow 2_1^+$ $E2$ transition, from:

$$q^2(E0/E2) = \rho^2(E0) \cdot \frac{\Omega_{E0}}{\alpha_{E2}} \cdot \frac{T_{1/2}}{\ln(2)} \tag{1}$$

where Ω_{E0} is the electronic factor for the $E0$ transition, α_{E2} is the internal conversion coefficient of the competing $E2$ transition, and $T_{1/2}$ is the half-life of the 0_2^+ state [26]. The $E0$ strength for $0_i^+ \rightarrow 0_f^+$ transitions decrease as a function of atomic mass, so it is reasonable to estimate a value in the region of 50 to 100 milliunits for ^{80,82}Sr [27]. Additionally, we estimate that the half-lives are on the order of a few ps, as the half-life of the 0_2^+ state has not been measured in ^{80}Sr and is only a large upper limit in ^{82}Sr [25].

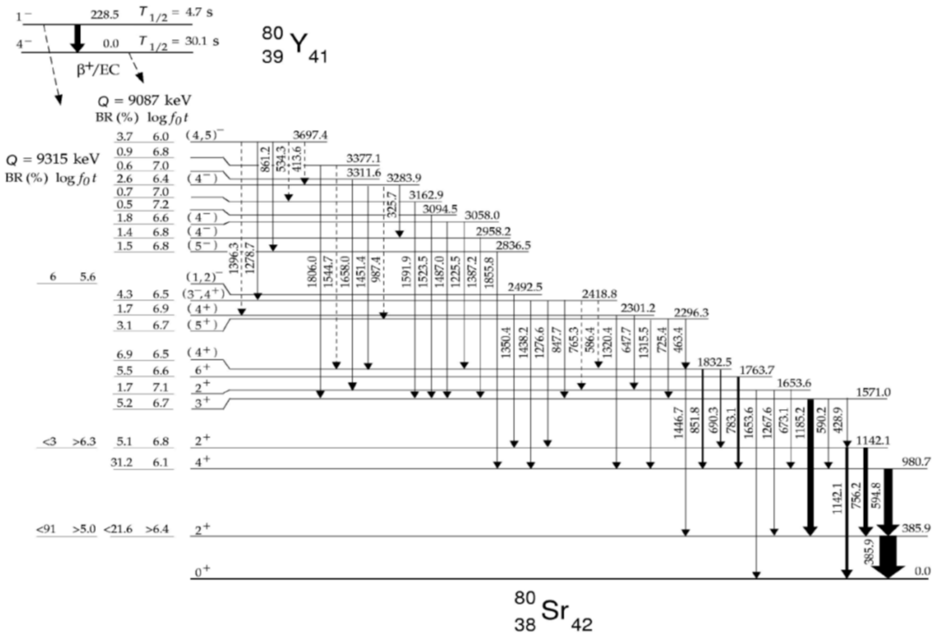

Figure 4: Partial decay scheme of ^{80}Sr. Arrow thicknesses correspond to relative transition intensities. Figure from Ref.[23].

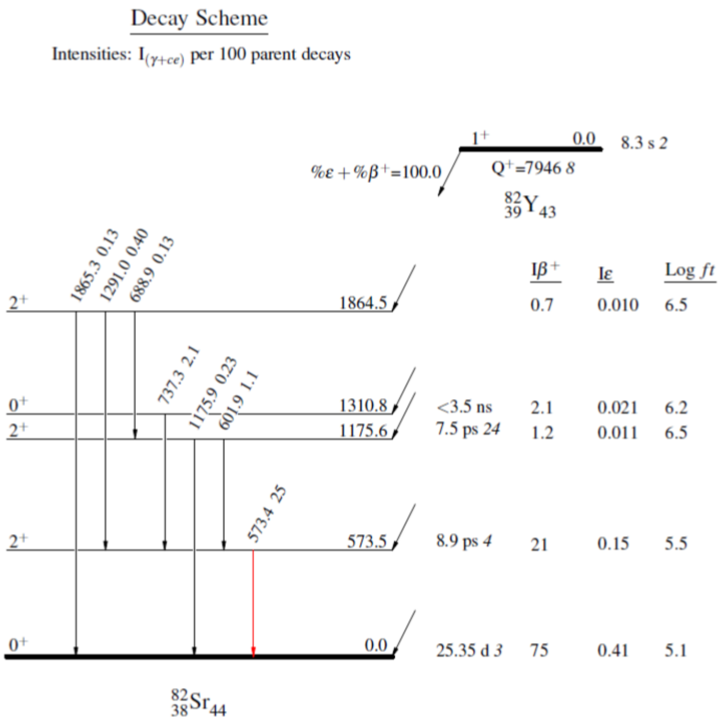

Figure 5: Low-lying levels of interest in ^{82}Sr. Figure from Ref. [24]. No transition probabilities are known for the 2_3^+ or 0_2^+ states and so they are excluded from rate calculations, however it is expected that they will be populated in the proposed measurement.

Table 1: Summary of the estimated yields for the (1^-) isomer in ^{80}Y and the ground state of ^{82}Y, the number of β-γ-γ coincidence counts for the four HPGe and two $LaBr_3$ detectors, the estimated number of $E0$ K conversion electrons in SPEDE, and the number of shifts requested. The number of $E2$ K conversion electrons is calculated to be about 10 times more than the $E0$ K conversion electrons [26]. To convert to ions/s, ions/μC are multiplied by a proton current of 2 μA.

Isotope	Half-life	Yield [ions/s]	β-γ_{Ge}-γ_{Ge} [counts/shift]	β-γ_{Ge}-γ_{LaBr} [counts/shift]	$E0$ e^- [counts/shift]	# of shifts
^{80}Y	4.8(3) s	1 x 10^4	$\sim$ 2 x 10^2	$\sim$ 1 x 10^2	40	9
^{82}Y	8.3(2) s	1 x 10^5	4 x 10^4	1 x 10^4	140	6

We propose to use $LaBr_3$(Ce) fast-timing detectors to measure the half-life of the states of interest using β-γ_{Ge}-γ_{LaBr} coincidences [28].

3 Experimental Facilities

The proposed β-decay experiment will use the ISOLDE Decay Station (IDS) setup [29] consisting of the tape station equipped with a fast plastic scintillator close to the implantation point having almost 25% efficiency for β detection, coupled to a combination of four HPGe clover-type detectors, two $LaBr_3$(Ce) detectors for fast-timing studies, and the SPEDE spectrometer [30] for internal conversion electron spectroscopy.
We propose to use two measurement positions: the implantation position where we have SPEDE and four clover detectors, and a decay position where we have the close configuration fast-timing setup with four clover and two $LaBr_3$ detectors. This will be achievable with the new IDS supporting structure (currently being manufactured). The isotopes will be implanted and measured at the first position for a period of time ($\sim$3 half-lives), then the implanted isotopes will be moved where the fast-timing measurement is performed for another $\sim$3 half-lives, while we continue to implant in the fresh tape at the implantation spot. The mixed measurement cycle means that half of the total measurement time will be at SPEDE and the other half for fast-timing. By sharing the activity between the two measurement positions, we can reproduce both the SPEDE and fast-timing configurations in their original forms and therefore preserving their efficiencies. Moreover, we can increase the performance of the fast-timing setup by adding more $LaBr_3$ detectors as there will be more space.
Pure YF_2^+ molecular beams will be produced from a Nb foil target equipped with a W surface ionizer and a CF_4 leak [32]. Refs [33, 34] show yields from the SC rather than from the PSB, however they do not quote a yield for the isomer of the ^{80}Y. Therefore, we request a first run of 3 shifts for yield confirmation from PSB and testing the equipment at IDS.
The estimated yields for ^{80,82}Y, the number of β-γ-γ coincidence counts for the relevant transitions in the HPGe and $LaBr_3$ detectors, the estimated number of conversion electrons in the SPEDE spectrometer, and the number of shifts requested for the proposed experiment are shown in the Table 1. The count rates are calculated using the

detection efficiency of the fast plastic scintillator (∼25%), the detection efficiency of four EUROBALL HPGe clovers in addback mode, and the detection efficiency of two $LaBr_3$ detectors at 14 mm.
Yields will be sufficient for significant population of the first and second excited states. Some population of the 0_2^+ state is also expected which will be used to infer shape coexistence. For ^{82}Sr, the coincidence rate is calculated for β particles in the plastic scintillator and the 574 ($2^+ \to 0^+$) and 737-keV ($0^+ \to 2^+$) γ-rays. Since the $0^+ \to 2^+$ transition has not been observed in ^{80}Sr yet, we estimate the coincidence rate using a transition intensity of 0.1%.
Since the conversion electrons for the $0^+ \to 0^+$ transitions in ^{80,82}Sr will have energies close to 1000 and 1310.8 keV (minus the binding energy of the electron), we will require a detector with a thickness larger than the standard 0.5 mm, which is optimised for electron energies up to 400 keV. The simulated detection efficiency of a 1-mm detector (3.5% at 1000 keV and 1.5% at 1300 keV) has been used in the rate estimations [29]. Thicknesses of up to 1.5 mm can be produced [30]. These shift estimates will allow an accurate measurement of the $E0/E2$ ratio with about 5% uncertainty [35].
To summarize, we propose to study the $E0$ transitions in ^{80,82}Sr using β^+/EC decay with the goal of expanding the systematics in the strontium isotopic chain. We will measure branching rations between low-lying states and will extract half-lives of exited states, in particular the excited the 0^+ states, which will help to shed light on the shape coexistence and shape evolution in this region.

Summary of requested shifts: We propose two separate runs: testing and data taking. Run 1: 1 shift to optimize the fluorination and ion source, 1 shift to measure different yields, and 1 shift for testing the equipment at IDS. Run 2: 9 shifts of ^{80}Y and 6 shifts of ^{82}Y from a Nb foil target with a CF_4 leak. In addition, we estimate the time needed to set up the beams to be 1 extra shift.

References

[1] C. J. Lister, B. J. Varley, H. G. Price and J. W. Olness, Phys. Rev. Lett **49** 308 (1982).

[2] C. J. Gross et al., Phys. Rev. C **39** 1780 (1989).

[3] C. J. Lister et al., Phys. Rev. C **42** R1191 (1990).

[4] P. J. Davies et al., Phys. Rev. C **75** 011302(R) (2007).

[5] S. M. Fischer et al., Phys. Rev. Lett. **13** 132501 (2001).

[6] T. A. Sienko, C. J. Lister and R. A. Kaye, Phys. Rev. C **67** 064311 (2003).

[7] J. Döring, et. al., Phys. Rev. C **59**, 59 (1999).

[8] M. Hasegawa et al., Phys. Lett. B **656** 51 (2007).

[9] A. Ahmed et al., Phys. Rev. C **24** 1486 (1981).

[10] J. H. Mamilton et al., Phys. Rev. Lett. **32** 239 (1974).

[11] J. Eberth et al., AI,P Conf. Proc. **164** 268 (1987).

[12] E. Clément et al. Phys. Rev. C **75** 054313 (2007).

[13] E. Bouchez et al., Phys. Rev. Lett. **90** 082502 (2003).

[14] F. Becker et al., Nucl. Phys. A 770 **107** (2006).

[15] W. Nazarewicz et. al., Nucl. Phys. A **435**, 397 (1985).

[16] A. Petrovici et al., Nucl. Phys. A **605** 290 (1996).

[17] Z. H. Wang et. al., J. Phys. G **42** 045108 (2015).

[18] J. Kantele et. al., Phys. A **289** 157 (1979).

[19] J.L. Wood et. al., Nucl. Phys. A **651** 323 (1999).

[20] C. J. Barton et. al., Phys. Rev. C **67** 034310 (2003).

[21] S. J. Zheng et al., Phys. Rev. C **90** 064309 (2014).

[22] P. Bonche et al., Nucl. Phys. A **443** 39 (1985).

[23] J. Doring et. al., Res. Natl. Inst. Stand. Technol. **105**, 43 (2000).

[24] J. K. Tuli, E. Browne., NDS **157** 260 (2019).

[25] Evaluated Nuclear Structure Data File (ENSDF), NNDC.

[26] T. Kibédi and R.H. Spear, Atomic Data and Nuclear Data Tables **89** 1, 77-100 (2005).

[27] L. J. Evitts et al., Phys. Rev. C **99** 024306 (2019).

[28] H. Mach, R. L. Gill, and M. Moszyński, Nucl. Instr. and Meth. in Phys. Res. A **280** 1 49-72 (1989).

[29] `https://isolde-ids.web.cern.ch/#setup`

[30] P. Papadakis et al., Eur. Phys. J. A **54** 42 (2018).

[31] V. N. Fedosseev et al., Hyperfine Int. **162** 15–27 (2005).

[32] H. Grawel et al., Zeitschrift für Physik A Hadrons and Nuclei **341** 247–248 (1992).

[33] R. Eder et al., Nucl. Instr. and Meth. in Phys. Res. B **62** 4 535-540 (1992).

[34] E. Hagebø et al., Nucl. Instr. and Meth. in Phys. Res. B **70** 1-4 165-174 (1992).

[35] J. N. Orce et al., J. Phys. G **31** 10 (2005).

Appendix

DESCRIPTION OF THE PROPOSED EXPERIMENT

The experimental setup comprises: (*name the fixed-ISOLDE installations, as well as flexible elements of the experiment*)

Part of the	Availability	Design and manufacturing
IDS	☒ Existing	☒ To be used with two $LaBr_3$(Ce) detectors and the SPEDE spectrometer

HAZARDS GENERATED BY THE EXPERIMENT (if using fixed installation:) Hazards named in the document relevant for the fixed IDS installation.

Additional hazards:

Hazards	$^{80,82}Y$		
Thermodynamic and fluidic			
Pressure	[pressure][Bar], [volume][l]		
Vacuum			
Temperature	[temperature] [K]		
Heat transfer			
Thermal properties of materials			
Cryogenic fluid	[fluid], [pressure][Bar], [volume][l]		
Electrical and electromagnetic			
Electricity	[voltage] [V], [current][A]		
Static electricity			
Magnetic field	[magnetic field] [T]		
Batteries	☐		
Capacitors	☐		
Ionizing radiation			
Target material [material]			
Beam particle type (e, p, ions, etc)			
Beam intensity			
Beam energy			
Cooling liquids	[liquid]		
Gases	[gas]		
Calibration sources:	☒		
• Open source	☐		

• Sealed source	☒ [ISO standard]		
• Isotope	^{56}Co, ^{60}Co, ^{133}Ba, ^{152}Eu		
• Activity			
Use of activated material:			
• Description	☐		
• Dose rate on contact and in 10 cm distance	[dose][mSV]		
• Isotope			
• Activity			
Non-ionizing radiation			
Laser			
UV light			
Microwaves (300MHz-30 GHz)			
Radiofrequency (1-300 MHz)			
Chemical			
Toxic	[chemical agent], [quantity]		
Harmful	[chem. agent], [quant.]		
CMR (carcinogens, mutagens and substances toxic to reproduction)	[chem. agent], [quant.]		
Corrosive	[chem. agent], [quant.]		
Irritant	[chem. agent], [quant.]		
Flammable	[chem. agent], [quant.]		
Oxidizing	[chem. agent], [quant.]		
Explosiveness	[chem. agent], [quant.]		
Asphyxiant	[chem. agent], [quant.]		
Dangerous for the environment	[chem. agent], [quant.]		
Mechanical			
Physical impact or mechanical energy (moving parts)	[location]		
Mechanical properties (Sharp, rough, slippery)	[location]		
Vibration	[location]		
Vehicles and Means of Transport	[location]		
Noise			
Frequency	[frequency],[Hz]		

Intensity			
Physical			
Confined spaces	[location]		
High workplaces	[location]		
Access to high workplaces	[location]		
Obstructions in passageways	[location]		
Manual handling	[location]		
Poor ergonomics	[location]		

Hazard identification:

Average electrical power requirements (excluding fixed ISOLDE-installation mentioned above): Negligible